Electronic Transitions of the Soret Band of Reaction Centers from *Rhodobacter sphaeroides* Studied by Femtosecond Transient Absorbance Spectroscopy

Haiyu Wang, Su Lin, and Neal W. Woodbury*

Department of Chemistry and Biochemistry, Arizona State University, and Biodesign Institute at Arizona State University, Tempe, Arizona 85287-5201

Received: August 26, 2005; In Final Form: February 6, 2006

The Soret band of reaction centers from *Rhodobacter sphaeroides* has been systematically studied using femtosecond transient absorption spectroscopy. When the excitation wavelength was scanned over the entire Soret band, the approximate absorption spectra of the bacteriochlorophyll dimer, the monomer bacteriochlorophylls, and the bacteriopheophytins within the Soret band were determined by analyzing the ground state bleaching with about 100 fs resolution. The main contribution of H is on the blue end of the spectrum, peaking near 350 nm, P absorbs mostly on the red side of the spectrum, but probably has multiple bands, and the main absorbance of B likely lies between H and P, overlapping with P on the red side (particularly near 390 nm). The energy transfer from B to P in the Q_Y band takes about 300 fs when Soret-band excitation is used and the time constant of overall energy transfer from H to B to P in the Q_Y band when H is specifically excited near 350 nm is about 500 fs. Internal conversion after Soret-band excitation is the rate-limiting step for the energy-transfer process. The time constant of internal conversion for B and P is less than 300 fs, and for H it is about 500 fs.

Introduction

The primary electron-transfer processes in photosynthesis take place in the reaction center, an integral membrane, pigment−protein complex. The structure and function of the reaction center from purple non-sulfur bacteria have been studied in detail, resulting in a fairly complete picture of the pathway and dynamics of photosynthetic electron transfer in this system.[1−6] The reaction center from *Rhodobacter sphaeroides* consists of three protein subunits—L, M, and H—and 10 cofactors: four bacteriochlorophylls (BChl), two bacteriopheophytins (BPheo), two quinone molecules, a caroteniod molecule, and a nonheme iron. The BChl, BPheo, and quinone cofactors are arranged in nearly symmetric branches.[7−10] These two branches (usually labeled A and B) each contain chemically identical cofactors, but the protein environment is not completely symmetric due to the amino acid differences between the heterodimer core subunits (L and M). The two pathways both start with a primary donor (P, a pair of BChls), followed by a monomer bacteriochlorophyll (either B_A or B_B), a bacteriopheophytin (either H_A or H_B), and then a ubiquinone (either Q_A or Q_B). Charge separation occurs almost exclusively along the A-side electron-transfer chain in wild-type reaction centers when either visible or near-infrared excitation is used.

One of the striking aspects of reaction center photochemistry that has recently become clear is that the pathway of electron transfer is wavelength-dependent.[11−16] For example, excitation directly into B rather than into the lowest transition of P has been shown to give rise to alternate photochemistry including direct formation of $P^+B_A^-$, particularly in certain reaction center mutants.[13] This suggests that energy transfer and electronic relaxation may not always precede electron transfer. More recently, excitation into the red side of the Soret band of the reaction center has been shown to give rise to fast transient formation of $B_B^+H_B^-$ at certain wavelengths.[15] This is particularly evident at low temperature or in certain mutants where $B_B^+H_B^-$ is relatively long-lived.[15,16]

Understanding these alternate electron-transfer reactions requires a clear understanding of the specific transitions excited throughout the reaction center spectrum. While the near-IR (Q_Y) and the visible (Q_X) bands of the reaction center are generally well understood in terms of what cofactors absorb at which wavelengths, the situation in the Soret band is much less clear. Figure 1 shows Soret band absorption spectra of the reaction centers at 10 and 298 K. H, B, and P all contribute to this band with two clear peaks located at 367 and 390 nm. A small shoulder can also be resolved at 350 nm, which is more pronounced at 10 K. The general electronic structure of the Soret band of both chlorophyll and pheophytin has been investigated previously, using theoretical and experimental approaches.[17,18] However, the assignment of H, B, and P transitions within the reaction center Soret band has not been performed experimentally. In this paper, by monitoring the instantaneous ground-state bleaching and stimulated emission that occurs as the wavelength of the excitation pulse is progressively scanned across the whole Soret band of the reaction center, profiles of the individual contributions of P, B, and H in this band have been generated. In addition, the pathway and kinetics of energy transfer that take place upon Soret-band excitation has also been explored.

Materials and Methods

Procedures for the preparation of His-tagged *Rhodobacter (Rb.) sphaeroides* reaction centers expressed from a pRK-based plasmid have been described previously.[19] For the transient absorbance change measurements, reaction centers were suspended in 15 mM Tris-HCl (pH 8.0), 0.025% *N*,*N*-dimethyldodecylamine-*N*-oxide (LDAO), 1 mM EDTA, 150 mM NaCl,

* Corresponding author. E-mail: Nwoodbury@asu.edu. Tel: 480-965-3294. Fax: 480-727-0396.

10.1021/jp054850i CCC: $33.50
Published on Web 03/10/2006

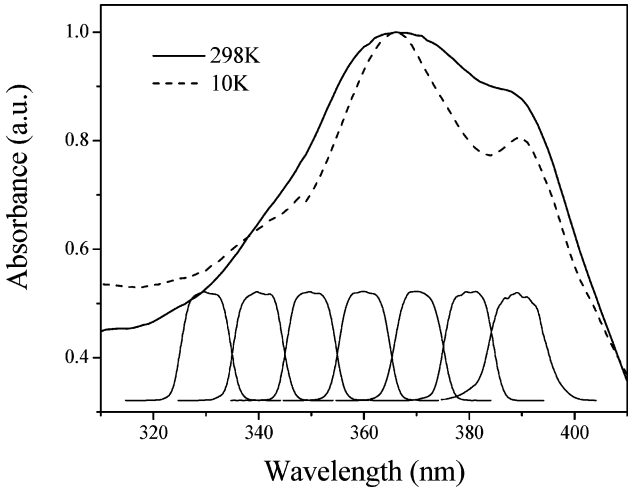

Figure 1. Soret-band absorbance spectrum of wild-type reaction centers at 298 and 10 K. Spectra of the excitation pulses used at each excitation wavelength are also shown.

and 0.1 mM orthophenanthroline. Samples were loaded into a spinning wheel with an optical path length of 1.2 mm. A final optical density of roughly 1.0 at 802 nm was used for all measurements.

The femtosecond transient absorbance measurements were performed as follows. A titanium sapphire oscillator (Tsunami, Spectra-Physics) was used to generate 100 fs, 800 nm laser pulses at a repetition rate of 82 MHz. These pulses were used to seed an optical amplifier system (Spitfire, Spectra-Physics), resulting in pulses of approximately 0.8 mJ at a kilohertz repetition rate. Part of the pulse energy (~10%) was then used to generate a white light continuum by focusing the beam into a sapphire plate and this was used for the probe beams. The remainder of the amplified 800 nm pulse was used to pump an optical parametric amplifier (OPA-800, Spectra-Physics) generating excitation pulses at wavelengths between 330 and 390 nm (fourth harmonic of the signal from the OPA). Transient absorption changes were measured from 730 to 950 nm using a monochromator (SP150, Action Res. Corp.) and a diode detector (Model 2032, New Focus Inc.). The time-resolved spectra were measured by scanning the monochromator at a particular time delay between the excitation and probe pulse. In this setup, timing inaccuracies due to wavelength-dependent dispersion effects between the excitation and probe pulses were directly corrected by adjusting the position of the optical delay line according to a calibration curve generated through measurement of the Kerr signal from CS_2. The relative polarization of the excitation and probe beams was set to the magic angle. The instrument response was nearly a Gaussian function in time. The fwhm of the instrument response changed slightly at different excitation wavelengths varying between 180 and 220 fs. After deconvolution the effective system time resolution was about 100 fs.

The excitation intensities were kept lower than 500 nJ per pulse for all measurements reported here, and the excitation spot size was about 1 mm in diameter. All the experiments were done at room temperature. Data analysis was carried out using locally written software (ASUFIT) developed under a MATLAB environment (Mathworks Inc., software available electronically upon request, ref 20).

Results

Figure 2 shows time-resolved spectra recorded at 100 fs, 500 fs, 1 ps, and 20 ps using excitation wavelengths of 350, 370, and 390 nm (complete time vs wavelength surfaces were collected for each of these excitation wavelengths as well as 330, 340, 360, and 380 nm and these data were used in the kinetic analyses described below and in Table 1). The spectra exhibit a significant excitation wavelength dependence. At all excitation wavelengths, at least part of the formation of the P-band bleaching at 865 nm does not occur instantaneously, and the appearance of bleaching at this wavelength is faster when excitation on the red side of the Soret band is used (see Figure 3a), implying that a larger fraction of the pulse energy on the longer wavelength side of the spectrum results in direct excitation of P than on the shorter wavelength side. Fitting the appearance of the P-band bleaching to an exponential function gives rise to a two component kinetic function in which a fraction of the bleaching appears instantly and part grows in with an exponential time constant. The exponential time constant ranges from 300 to 500 fs, depending on the excitation wavelength. The fraction of the bleaching that occurs instantaneously is also excitation wavelength-dependent. The results are summarized in Table 1. The slowest kinetics are found with 350 nm laser excitation and at this wavelength 30% of the P bleaching occurs instantaneously while the remaining 70% of the bleaching forms with a time constant of 500 fs. When the

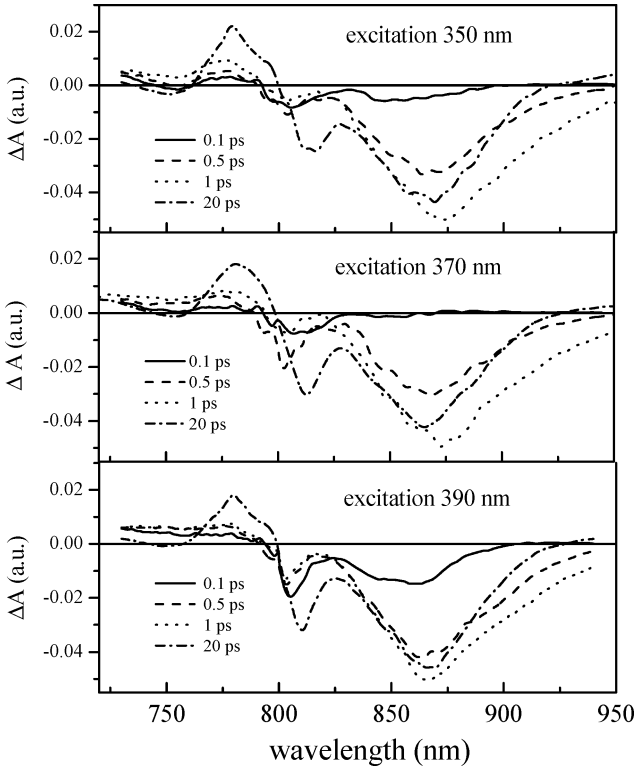

Figure 2. Time-resolved spectra of the reaction center Q_Y band at 100 fs, 500 fs, 1 ps, and 20 ps using excitation at 350 nm (top), 370 nm (middle), and 390 nm (bottom).

TABLE 1: Kinetic Analysis of the Initial Bleaching of the Ground-State Absorbance Band of P Measured at 865 nm

excitation (nm)	τ (fs)	A (%)	instantaneous P formation (%)
330	410 ± 50	100 ± 5	0 ± 5
340	380 ± 40	99 ± 5	1 ± 5
350	510 ± 60	70 ± 20	30 ± 20
360	300 ± 30	100 ± 6	0 ± 6
370	390 ± 46	90 ± 22	10 ± 22
380	310 ± 30	47 ± 11	53 ± 11
390	340 ± 35	33 ± 8	67 ± 8

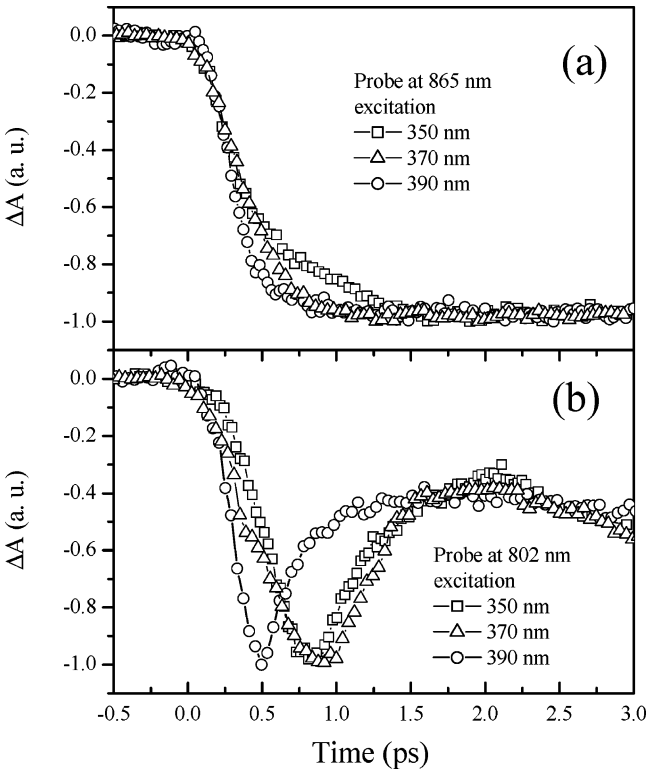

Figure 3. Time-dependent changes in the absorbance spectra using 350, 367, or 390 nm excitation at two different detection wavelengths: (a) 865 nm (ground-state absorbance band of P) and (b) 802 nm (ground-state absorbance band of the monomer bacteriochlorophylls, B_A and B_B).

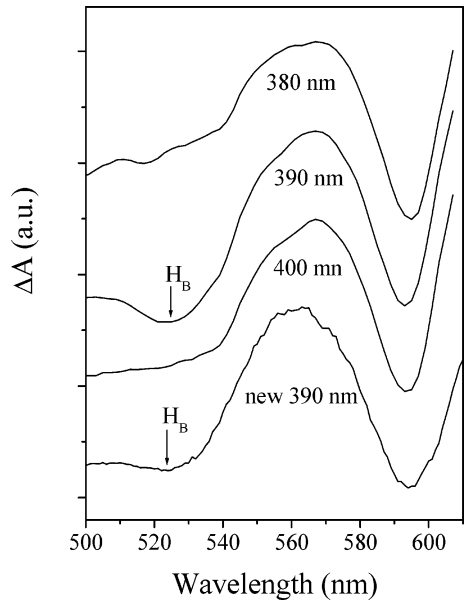

Figure 4. Time-resolved spectra of the reaction center Q_X band at 800 fs. The top three spectra were measured using the transient absorbance apparatus of ref 15 with excitation wavelengths of 380, 390, and 400 nm, as shown. The spectral profiles of the laser pulses from that system are about 2.5 nm wide (fwhm). The bottom spectrum was measured by the current transient absorbance apparatus using excitation at 390 nm (excitation fwhm of about 10 nm). The spectra were normalized at the P/B bleaching around 595 nm. The wavelength of H_B bleaching is indicated.

excitation is moved to 340 or 330 nm, P is not directly excited at all (Table 1); however, the exponential time constant for the formation of P bleaching is somewhat faster (about 400 fs). At 390 nm excitation, 70% of P is directly excited.

The large fraction of P directly excited using 390 nm excitation was quite unexpected given our previous measurements using a different setup that indicated that P formation was slow compared to B formation using 390 nm excitation.[15] In addition, we observe less of the fast transient formation of $B_B^+H_B^-$ than was observed in the previous 390 nm excitation experiments. $B_B^+H_B^-$ is formed within a few hundred femtoseconds of excitation and results in a transient bleaching near 530 nm that decays on the picosecond time scale. Figure 4 compares Q_X-region transient difference spectra at 800 fs measured by the previous transient absorbance setup used in ref 15 (380, 390, and 400 nm excitation wavelengths) and the current setup (390 nm excitation); the H_B bleaching associated with $B_B^+H_B^-$ is significantly less than that seen in the previous result (about $^1/_3$ the amplitude, as determined by comparing the difference in absorbance signals at 510 and 530 nm). The most likely explanation for this discrepancy stems from the spectral pulse width used in the previous study (2.5 nm) compared to that used in the current study (about 10 nm) (Figure 1). Apparently, the narrow excitation region at 390 nm in the previous experiments resulted in a larger fraction of B* rather than P*. Note that, in the earlier measurements, 380 and 400 nm excitation gave rise to almost no B-side charge separation, suggesting that the spectral region in which B-side charge separation occurs (a region where P is presumably not excited to a large extent) is quiet narrow (Figure 4). Thus, 390 nm excitation appears to be very special in this regard, as B-side charge separation has not been observed at any other wavelength in the Soret band. The excitation wavelength dependence of $B_B^+H_B^-$ formation is now being investigated in more detail using a mutant that forms a long-lived $B_B^+H_B^-$ state at room temperature.[16] Both the current measurements and previous measurements are consistent in general as they both have shown slower formation of P-band bleaching upon shifting the excitation wavelength to the blue of 380 nm.

The kinetics probed at 930 nm is dominated by the stimulated emission from P*. The formation of P* occurs on a time scale of several hundred femtoseconds, nearly the same as that of P-band bleaching (probed at 860 nm), and again the slowest P* formation is observed using 350 nm excitation (Table 2). The decay of the stimulated emission in each case can be well fitted by two exponential components with exponential time constants (and relative amplitudes) of 3.3 ps (90%) and 11 ps (10%). This is consistent with previous results by transient absorption and also up-conversion measurements using direct excitation of P[21,22] and is thus not wavelength-dependent (the same decay kinetics is observed when exciting P in the Soret band as is observed when exciting at 860 nm directly into the lowest excited singlet state of P). This nonexponential decay can be explained by either a homogeneous sample with multiple distinct interacting states[21] or a static inhomogeneous distribution of rates.[22]

There is also a wavelength dependence to the B-band bleaching near 802 nm when exciting at various positions in the Soret band. As the excitation wavelength is moved to the red side of the Soret band, the amplitudes of the B-band bleaching increase and the buildup of B-band bleaching (802 nm) is faster. When 390 nm excitation is used, the appearance of the 802 nm transient is instantaneous. When other excitation wavelengths are used, at least part of the bleaching at 802 nm grows in more slowly (roughly 500 fs) (Figure 3b). When 370 nm excitation is used, the growth of the bleaching within the first 500 fs is faster than that with 350 nm excitation (Figures 2 and 3b), suggesting that there is progressively more direct

TABLE 2: Kinetic Analysis of Transient Absorbance Measured at 930 nm (the Stimulated Emission from P*)

excitation (nm)	τ_1 (fs)	A_1 (%)	τ_2 (ps)	A_2 (%)	τ_3 (ps)	A_3 (%)
330	400 ± 50	−100 ± 5	3.4 ± 0.5	90 ± 4	10 ± 2	10 ± 4
340	400 ± 40	−100 ± 5	3.5 ± 0.5	90 ± 3	11 ± 2	10 ± 3
350	500 ± 60	−95 ± 10	3.3 ± 0.5	90 ± 2	11 ± 2	10 ± 2
360	320 ± 40	−100 ± 5	3.5 ± 0.5	90 ± 2	11 ± 2	10 ± 2
370	400 ± 50	−100 ± 15	3.3 ± 0.5	90 ± 3	11 ± 2	10 ± 3
380	340 ± 40	−100 ± 10	3.4 ± 0.5	90 ± 3	10 ± 2	10 ± 3
390	350 ± 30	−100 ± 7	3.3 ± 0.5	90 ± 2	11 ± 2	10 ± 2

excitation of B as the excitation wavelength is moved toward the longer wavelength side of the Soret band.

The bleaching of the H band near 760 nm is also excitation wavelength-dependent. In a comparison of the early time (100 fs) spectra taken using different excitation wavelengths, it is clear that the H transition is located on the blue side of the Soret band (Figure 2). When 390 nm excitation is used, almost no bleaching of the 760 nm H band is seen at all. In contrast, excitation at 350 nm gives rise to an initial bleaching of the H band (100 fs) that has almost the same amplitude as does the bleaching due to the formation of the H anion of the charge-separated state $P^+H_A^-$ present at 20 ps. This indicates that essentially all of the charge-separated state formed comes from excitation of H and therefore neither B nor P is appreciably excited at 350 nm. Note that the transients in the 730−770 nm region generally have a positive absolute absorbance change at early times due to excited state absorption. However, the initial bleaching of the 760 nm H band is clearly present on top of this absorbance increase when excitation near the blue end of the Soret band is used.

Even after charge separation is complete (the 20 ps spectra in Figure 2), the difference spectra still exhibit excitation wavelength-dependence. Similar results have been observed previously using direct excitation of H, B, and P in the Q_Y region of the reaction center spectrum.[23−25]

Discussion

Energy Transfer and Internal Conversion. The ultrafast energy transfer between H, B, and P in bacterial reaction centers has been previously studied by femtosecond transient absorption spectroscopy, as well as by fluorescence up-conversion methods.[24−28] Upon direct excitation of the lowest excited singlet states of these cofactors, the H to B energy transfer occurs within 100 fs and the energy transfer from B to P occurs in 100−150 fs. Excitation into the Soret band results in formation of higher excited states. In this case, there are two possible energy-transfer pathways. First, it is possible for the electron to relax to the lowest excited state by ultrafast internal conversion with subsequent transfer among H, B, and P by previously observed mechanisms. Alternatively, it is possible for energy transfer to occur directly from the higher excited state if transfer is fast enough compared to relaxation. For example, the energy transfer from carotenoid to chlorophyll or bacteriochlorophyll in photosynthetic systems occurs both ways, and transfer from the S_2 excited state sometimes dominates.[29,30]

The transients associated with energy transfer between B and P after exciting the Soret band of the reaction center are shown in Figure 3. The delayed formation of the P-band bleaching (the part of the 865 nm bleaching that is not instantaneous) occurs with essentially the same kinetics as the recovery of the B-band bleaching at 802 nm using either 390 or 350 nm excitation, though the makeup of the initial excited-state population in terms of P*, B*, and H* changes dramatically between 390 and 350 nm. On the red side of the Soret band (390 nm), initial excitation results in a mixture of P* and, to a lesser extent, B*. Fitting of the absorbance change signals generated by 390 nm excitation gives a good estimate of the B to P energy-transfer rate constant under these excitation conditions (the slow part of the P formation is small, but there is little excitation of H at this wavelength, making the analysis simpler). This fit results in a 340 fs time constant. In fact, in general for Soret-band excitation, the part of the kinetics associated with B to P energy transfer has a kinetic time constant of about 300 fs. Recently, the S_3 state (Soret band) of bacteriochlorophyll in pyridine solution has been shown to have a lifetime of about 260 fs by fluorescence depletion spectroscopy.[31] Thus, one explanation of the 300 fs time constant for energy transfer from B to P upon Soret-band excitation is that the internal conversion is rate-limiting (B to P energy transfer has been shown previously to occur in 100−150 fs from the lowest excited state) and that most of the energy transfer between B and P upon the Soret-band excitation occurs from the lowest excited state (Q_Y band) after internal conversion. However, one cannot rule out direct energy transfer from the higher excited state of B to P occurring within the time resolution of the instrument.

When the blue side of the Soret band is excited (350 nm), the initial excited singlet state formed is almost exclusively an excited state of H and any energy transfer must occur either directly or indirectly from this initial state. Bleaching of the 802 nm transition (the B band, see Figure 3b) upon 350 nm excitation is delayed by about 500 fs. This is much slower than the H to B energy transfer process observed upon direct excitation of H in the Q_Y band (less than 100 fs). While, as with B to P energy transfer, it is not possible to rule out very fast direct energy transfer from H to B from the higher excited state of H, one consistent model is that internal conversion of the upper excited state of H is rate-limiting, and this internal conversion occurs on the 400−500 fs time scale. As shown in Figure 2, there is very little bleaching of the B band seen at early times at all. This is because H to B energy transfer is slower than B to P energy transfer, resulting in only a low steady-state population of excited B. This makes it difficult to reliably fit the process using a kinetic model for H to B to P energy transfer. For this reason it was not possible to generate quantitative rate constants for the individual steps.

Excitation at 370 nm (which likely excites a mixture of H and B, see below) results in decay kinetics that are similar to those obtained upon 350 nm excitation, again probably reflecting internal conversion of the higher excited state of H followed by H to B energy transfer (Figure 3). However, there is a small, but significant kinetic difference between the two excitation wavelengths. Using 370 nm excitation, the bleaching at 802 nm (B band) grows in more rapidly initially than is seen using 350 nm excitation (Figure 3B). As a result, the transient population of B* is higher than that seen for 350 nm excitation. The fact that the H excited states formed using 350 vs 370 nm excitation give rise to somewhat different kinetic traces suggests

that the proportion of H_A vs H_B excited at 350 vs 370 nm may be different. It is possible that the observed kinetics represents a mixture of internal conversion and very fast direct energy transfer from the higher excited state and that the relative amount of these two processes is different for the two different bacteriopheophytins.

By comparing the absorbance change transients associated with P-bleaching and P*-stimulated emission (Q_Y band), it is possible to put limits on the internal conversion time of P. The best fitting results show the formation of P* has essentially the same time constant as that of P bleaching when it is formed via energy transfer, ranging from 300 to 500 fs, depending on the excitation wavelength. For 390 nm excitation, which primarily excites the P band directly, nearly 100% of P* is formed within a time constant of about 350 fs. No additional slower dynamics are observed, meaning that the internal conversion after Soret-band excitation of P takes place in 300 fs or less.

H, B, and P Soret-Band Contributions. Analysis of the early time spectra as a function of excitation wavelength clearly indicate that the Soret transition associated with the bacteriopheophytins in the reaction center is located on the blue side of the Soret band. Excitation at 390 nm in the Soret band results in no contribution from excited H at all (no initial ground-state bleaching of H, Figure 2). When 350 nm laser excitation is used, the initial bleaching of the H band (100 fs) has almost the same amplitude as it does after charge separation is complete (at 20 ps), implying that the dominant excited state using 350 nm excitation is that of H. It should be noted that the Soret band has a small shoulder at 350 nm (more pronounced at low temperature), and thus this shoulder is probably associated with one peak of the H−Soret band (Figure 1). By considering the initial bleaching of the H band as a function of excitation wavelength, it is possible to determine the relative absorption characteristics for the bacteriopheophytins in the Soret band. Because the early time excited-state absorption between 720 and 780 nm is nearly flat, the initial bleaching of the H band at 100 fs can be determined by comparing the difference in absorbance signals at 720 and 760 nm. By normalizing the bleaching with respect to the amplitude of the final Q_Y-band bleaching of P, it is possible to calculate a relative contribution of the H transition to the absorbance, as shown in Figure 5a. It may be that the actual amplitude of the 370 nm H absorbance is larger than that shown in Figure 5a; the very fast energy transfer between H and B at this excitation wavelength tends to minimize the size of the early time bleaching of H.

The dynamics of the initial bleaching of the P band, and corresponding formation of P*, reflect the relative contribution of P absorbance at different wavelengths in the Soret band. P* formation becomes faster as the excitation wavelength progresses toward the red side of the Soret band (see Figure 3a), which implies that more P is directly excited on the red edge. The fraction of P that is directly excited increases as the excitation wavelength is changed from 350 to 390 nm. As discussed above, the processes occurring on the few hundred femtosecond time scale reflect energy transfer between B and P or among H, B, and P. The fitting results of Table 1 provide the information required to determine how much of the P band is directly excited (the instantaneous part) at each point in the absorption spectrum of the Soret band. A relative measure of the absorbance contribution of the P band can be obtained at each point in the Soret band by multiplying the total Soret-band absorbance at each wavelength by the fraction of the P bleaching that occurred instantaneously (Figure 5b). Both P and H absorbance show

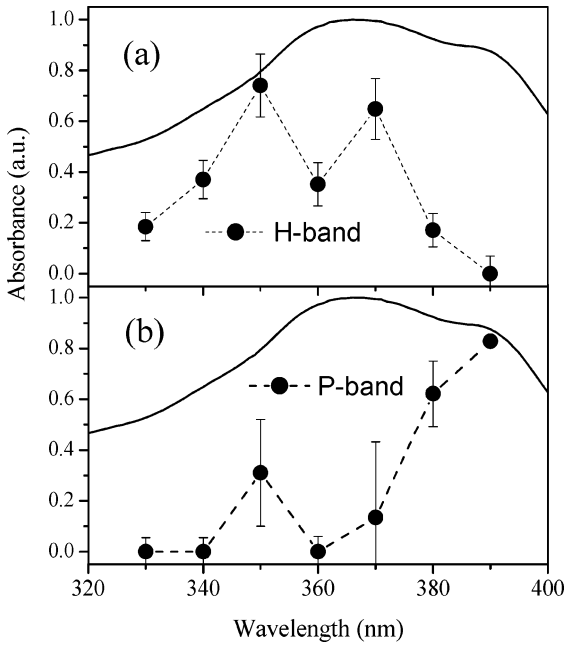

Figure 5. H (panel a) and P (panel b) relative absorbance contributions to the Soret band of wild-type reaction centers extracted from femtosecond transient absorbance spectra with 100 fs time resolution, as described in the text. The solid line is the Soret-band absorbance spectrum of wild-type reaction centers in each panel.

two maxima in their absorbance profiles. The Soret bands of BChl and BPheo in solution are known to exist in two similar energy states, B_X and B_Y.[32,33] Another possible source of the multiple Soret bands for P and H may be the differences between the two sides of the reaction center.

Unfortunately, it is difficult to determine the amplitude of the initial bleaching of the ground state of B accurately because B serves as both an energy donor and acceptor (with formation and decay on similar time scales), making the kinetic resolution of the spectrum very unreliable. However, the amplitude of B-band bleaching obviously decreases as the excitation wavelength moves toward the blue. This implies that the B band is red-shifted relative to the H band. This agrees with previous experimental and theoretical work on the electronic states of chlorophyll and pheophytin. The chlorophyll Soret band is slightly red-shifted relative to that of pheophytin.[17,18] It is likely that B is located between H and P in the Soret band, contributing to both the 390 nm shoulder as well as to the 370 nm region.

After charge separation is largely complete (10 ps), the H and B Q_Y bands continue evolving over approximately 30 ps. Part of this evolution may reflect the vibrational cooling process since a large amount of excessive vibrational energy is released during internal conversion (about 15000 cm^{-1}) and vibrational cooling typically has a time scale on the order of 10 ps.[34−36] The transient spectra even at 20 ps exhibit a clear excitation wavelength-dependence (Figure 2). In a comparison of excitation at 350 nm (mostly H) and 390 nm (mostly P and B), H-band bleaching at 20 ps is more pronounced using 350 nm excitation. This is consistent with earlier results comparing 760 nm excitation (H excitation) to 860 nm excitation (P excitation).[24] This suggests that while Soret-band excitation is selective with regard to cofactor excitation, there is no additional effect of Soret-band excitation on the long-lived states formed in the reaction center.

Conclusions

With scanning of the excitation wavelength between 330 and 390 nm and monitoring of the early time absorbances changes,

the approximate absorption spectra of H, B, and P within the Soret band have been determined. The contribution of the H transitions peak near 350 and 370 nm. In contrast, P absorbs on the red side of the Soret band. The B band is not clearly separated from the other two in fits, and thus can only be qualitatively evaluated. The main absorbance apparently lies between H and P, overlapping with P on the red side (particularly near 390 nm). In a comparison of the amount of B-side charge separation ($B_B^+H_B^-$ formation) upon 390 nm excitation that was observed in earlier studies using spectrally very narrow excitation with the amount of B-side charge separation observed here (using excitation pulses that are spectrally several times broader), less B-side charge separation is observed in the current work (about $^1/_3$ as much), suggesting that B-side charge separation occurs only over a spectrally narrow window of excitation wavelengths. The energy transfer from B to P in the Q_Y band takes about 300 fs using Soret-band excitation, and the time constant of overall energy transfer from H to B to P in the Q_Y band when H is specifically excited near 350 nm is about 500 fs. The energy-transfer processes probably take place from the lowest excited states of either B or H, with the internal conversion process that occurs after Soret-band excitation being the rate-limiting step, though it is not possible to exclude some energy transfer directly from the higher excited state with a very fast rate constant (less than 100 fs). When this model is used, the time constant of internal conversion starting with Soret-band excitation of B and P is less than 300 fs; for H it is about 500 fs.

Acknowledgment. We thank Carole Flores and Dr. Evaldas Katilius for their help with the reaction center preparation. This research was supported by NSF Grant MCB0131776. The transient spectrometer used was funded by NSF Grant BIR9512970. This is publication #650 from the Center for the Study of Early Events in Photosynthesis, Arizona State University.

References and Notes

(1) Parson, W. W. In *Protein Electron Transfer*; Bendall, S. D., Ed.; BIOS Scientific Publishers: Oxford, 1996; pp 125−160.

(2) Woodbury, N. W.; Allen, J. P. In *Anoxygenic Photosynthetic Bacteria*; Blankenship, R. E., Madigan, M. T., Bauer, C. E., Eds.; Kluwer Academic Publishers: Dordrecht, 1995; Vol. 2, pp 527−557.

(3) Okamura, M. Y.; Paddock, M. L.; Graige, M. S.; Feher, G. *Biochim. Biophys. Acta* **2000**, *1458*, 148−163.

(4) Kirmaier, C.; Holten, D. In *The Photosynthetic Reaction Center*; Deisenhofer, J., Norris, J. R., Eds.; Academic Press: San Diego, 1993; pp 49−70.

(5) Martin, J.-L.; Vos, M. H. *Annu. Rev. Biophys. Biomol. Struct.* **1992**, *21*, 199−222.

(6) Zinth, W.; Kaiser, W. In *The Photosynthetic Reaction Center*; Deisenhofer, J., Norris, J. R., Eds.; Academic Press: San Diego, 1993; pp 71−88.

(7) Deisenhofer, J.; Epp, O.; Miki, K.; Huber, R.; Michel, H. *J. Mol. Biol.* **1984**, *180*, 385−398.

(8) Ermler, U.; Fritzsch, G.; Buchanan, S. K.; Michel, H. *Structure* **1994**, *2*, 925−936.

(9) Allen, J. P.; Feher, G.; Yeates, T. O.; Komiya, H.; Rees, D. C. *Proc. Natl. Acad. Sci. U.S.A.* **1987**, *84*, 5730−5734.

(10) Chang, C.-H.; El-Kabbani, O.; Tiede, D.; Norris, J.; Schiffer, M. *Biochemistry* **1991**, *30*, 5352−5360.

(11) Van Brederode, M. E.; Jones, M. R.; Van Mourik, F.; Van Stokkum, I. H. M.; Van Grondelle, R. *Biochemistry* **1997**, *36*, 6855−6861.

(12) Zhou, H. L.; Boxer, S. G. *J. Phys. Chem. B* **1998**, *102*, 9139−9147.

(13) Van Brederode, M. E.; Van Stokkum, I. H. M.; Katilius, E.; Van Mourik, F.; Jones, M. R.; Van Grondelle, R. *Biochemistry* **1999**, *38*, 7545−7555.

(14) Lin, S.; Jackson, J. A.; Taguchi, A. K. W.; Woodbury, N. W. *J. Phys. Chem. B* **1999**, *103*, 4757−4763.

(15) Lin, S.; Katilius, E.; Haffa, A. L. M.; Taguchi, A. K. W.; Woodbury, N. W. *Biochemistry* **2001**, *40*, 13767−13773.

(16) Haffa, A. L. M.; Lin, S.; Williams, J. C.; Taguchi, A. K. W.; Allen, J. P.; Woodbury, N. W. *J. Phys. Chem. B* **2003**, *107*, 12503−12510.

(17) Fragata, M.; Norden, B.; Kurusev, T *Photochem. Photobiol.* **1988**, *47*, 133−143.

(18) Parusel, A. B. J.; Grimme S. *J. Phys. Chem. B* **2000**, *104*, 5395−5398.

(19) Goldsmith, J. O.; Boxer, S. G. *Biochim. Biophys. Acta* **1996**, *1276*, 171−175.

(20) Katilius, E.; Turanchik, T.; Lin, S.; Taguchi, A. K. W.; Woodbury, N. W. *J. Phys. Chem. B* **1999**, *103*, 7386-7389.

(21) Huber, H.; Meyer, M.; Scheer, H.; Zinth, W.; Wachtveitl, J. *Photosynth. Res.* **1998**, *55*, 153−162.

(22) Du, M.; Rosenthal, S. J.; Xie, X. L.; Dimagno, T. J.; Schmidt, M.; Hanson, D. K.; Schiffer, M; Norris, J. R.; Fleming, G. R. *Proc. Natl. Acad. Sci. U.S.A.* **1992**, *89*, 8517−8521.

(23) Peloquin, J. M.; Lin, S.; Taguchi, A. K. W.; Woodbury, N. W. *J. Phys. Chem.* **1996**, *100*, 14228−14235.

(24) Lin, S.; Taguchi, A. K. W.; Woodbury, N. W. *J. Phys. Chem.* **1996**, *100*, 17067−17078.

(25) Lin, S.; Jackson, J.; Taguchi, A. K. W.; Woodbury, N. W. *J. Phys. Chem. B* **1998**, *102*, 4016−4022.

(26) Stanley, R. J.; King, B.; Boxer, S. G. *J. Phys. Chem.* **1996**, *100*, 12052−12059.

(27) Vos, M. H.; Breton, J.; Martin, J.-L. *J. Phys. Chem. B* **1997**, *101*, 9820−9832.

(28) King, B. A.; McAnaney, T. B.; deWinter, A.; Boxer, S. G. *J. Phys. Chem. B* **2000**, *104*, 8895−8902.

(29) Lin, S.; Katilius, E.; Taguchi, A. K. W.; Woodbury, N. W. *J. Phys. Chem. B* **2003**, *107*, 14103−14108.

(30) Polivka, T.; Sundstrom, V. *Chem. Rev.* **2004**, *104*, 2021−2071.

(31) Shi, Y.; Liu, J. Y.; Han, K.; Lou, N. Q. *Chin. J. Chem. Phys.* **2004,** *17*, 1−3.

(32) Scherz, Z.; Parson, W. W. *Biochim. Biophys. Acta* **1984**, 766, 653−665.

(33) Hoff, A. J. *Phys. Rep.* **1997**, 287, 1−247.

(34) Ohta, K.; Kang, T. J.; Tominaga, K.; Yoshihara, K. *Chem. Phys.* **1999**, *242*, 103−114.

(35) Kovalenko, S. A.; Schanz, R.; Henning H.; Ernsting, N. P. *J. Chem. Phys.* **2001**, *115*, 3256−3273.

(36) Wang, H.; Zhang, H.; Abou-Zied, O. K.; Yu, C.; Romesberg, F. E.; Glasbeek, M. *Chem. Phys. Lett.* **2003**, *367*, 599−608.